Available online at www.sciencedirect.com
ScienceDirect
Planetary and Space Science 56 (2008) 2009–2025
Planetary and Space Science
www.elsevier.com/locate/pss

Simulating Martian regolith in the laboratory

Karsten Seiferlin[a,*], Pascale Ehrenfreund[b], James Garry[b], Kurt Gunderson[a], E. Hütter[c], Günter Kargl[c], Alessandro Maturilli[d], Jonathan Peter Merrison[e]

[a]*Physikalisches Institut, Universität Bern, Sidlerstrasse 5, 3012 Bern, Switzerland*
[b]*Astrobiology Laboratory, Leiden Institute of Chemistry, P.O. Box 9502, 2300 RA Leiden, The Netherlands*
[c]*Institut für Weltraumforschung, Graz, Österreichische Akademie der Wissenschaften, Austria*
[d]*German Aerospace Centre (DLR), Institute for Planetary Research, Rutherfordstr. 2, 12489 Berlin-Adlershof, Germany*
[e]*Aarhus Mars Simulation Laboratory, Aarhus University, Denmark*

Received 6 December 2007; received in revised form 21 July 2008; accepted 21 September 2008
Available online 15 October 2008

Abstract

Regolith and dust cover the surfaces of the Solar Systems solid bodies, and thus constitute the visible surface of these objects. The topmost layers also interact with space or the atmosphere in the case of Mars, Venus and Titan. Surface probes have been proposed, studied and flown to some of these worlds. Landers and some of the mechanisms they carry, e.g. sampling devices, drills and subsurface probes (“moles”) will interact with the porous surface layer. The absence of true extraterrestrial test materials in ample quantities restricts experiments to the use of soil or regolith analogue materials. Several standardized soil simulants have been developed and produced and are commonly used for a variety of laboratory experiments. In this paper we intend to give an overview of some of the most important soil simulants, and describe experiments (penetrometry, thermal conductivity, aeolian transport, goniometry, spectroscopy and exobiology) made in various European laboratory facilities.

Keywords: Martian soil; Lunar soil; Soil simulants; JSC-1; Salten Skov; Thermal conductivity

1. Introduction

Mars, the Moon, Mercury and many other solar system objects (e.g. asteroids, satellites) are covered by a layer of (mostly) loose, granular material, which is called *regolith*. Martian regolith is frequently, but nevertheless incorrectly, called *soil* (*soil* is a pedogenetic term reserved for Earth, and requires chemical, mineralogical and structural modifications induced by intense biological activity). The regolith layer constitutes the visible surface of these objects, determines the energy balance with the sky (open space or atmospheric) and interacts mechanically with impacting meteorites, surface landers, rovers, drills and sampling devices. On Mars it may exchange volatiles with the atmosphere and it interacts with wind. A layer of regolith can serve as a thermal blanket for near-surface ices, modifying their mobility and thermomechanical properties. Such a layer may also bear organic molecules arising from indigenous or exogenous processes: a regoliths fine-structure and large specific surface area provides some shielding from solar ultraviolet (UV) light that can degrade organic matter. Sufficiently thick layers of regolith can attenuate cosmic radiation.

One of the objectives of international future planetary exploration programs is to implement a long-term plan for the robotic and human exploration of solar system bodies. The Moon has recently attracted renewed interest by space agencies, e.g. NASA’s “Moon Mars and Beyond” and ESA’s *Aurora* programme. Mars has been a central object of interest in the context of extraterrestrial life. In support of future missions to Mars, simulations in the laboratory are crucial to optimize *in situ* exploration and measurements. Simulations of the Martian environment can focus on instrument testing, measurements on planetary analogues, or address planetary protection issues, for instance. All these are vital in support of planetary exploration. Even when *exploration* aspects are not considered, Mars and its

*Corresponding author. Tel.: +41 31 6314415.
E-mail address: karsten.seiferlin@space.unibe.ch (K. Seiferlin).

0032-0633/$ - see front matter © 2008 Elsevier Ltd. All rights reserved.
doi:10.1016/j.pss.2008.09.017

surface are interesting research subjects of their own right for planetary scientists. Many fields of planetary research necessitate having an understanding of the nature of a regolith and the physical and chemical processes occurring in a planetary environment. Apart from modeling and *in situ* measurements, laboratory experiments are a potential tool to investigate regoliths. Whether properties of the soil itself and processes therein are in the focus of such experiments or whether a test bed for space instrumentation is needed—the choice of a good sample material is crucial. Results and conclusions drawn from simulation experiments depend on the sample material that is used. True extraterrestrial samples are either not available at all or are too precious to be consumed (i.e. modified and contaminated) by simulation experiments. Even if returned samples would be available in ample quantities, they would in some cases, like, for example, thermal properties measurements, not be a good sample material: the simple fact that the samples had to be removed from their natural environment would modify their microstructure, their humidity, their natural temperature field, the ambient pressure within the pores and other key parameters (see Section 5). This adds to the necessity for good analogues as well as good simulation facilities.

In this paper we will provide a short overview of some commonly used soil analogues, followed by summaries of studies that have been made with these materials in various European laboratories. The experiments described in this paper and the involved laboratories are by no means comprehensive, and the selection we had to make should not be understood as a discrimination of those not included. Several other groups—in Europe and beyond—contribute substantially to space simulation experiments using soil simulants. Recent Mars missions provided a great wealth of knowledge about different Martian soil types (see Banin, 2005; Bell et al., 2000; Herkenhoff et al., 2004; Johnson et al., 2007; Richter et al., 2006; Soderblom et al., 2004, for example). We will, wherever possible, compare our findings about Martian analogues with *in situ* measurements. Because of the diversity of experiments that are described below, there are no coherent conclusions which would connect the various chapters with each other, and we defer the conclusions from the end of the paper to the individual chapters. Table 1 outlines the paper and associates sections with their authors and the laboratories and facilities used.

Table 1
Paper outline: chapters, associated laboratories and facilities, authors

Chapter 3: Penetrometry: Institut für Weltraumforschung, Graz
Chapter 4: Aeolian transport of Martian dust: Aarhus Mars Simulation Laboratory, Aarhus
Chapter 5: Thermal conductivity: Physikalisches Institut, Universität Bern, and Institut für Weltraumforschung, Graz
Chapter 6: Goniometry: Physikalisches Institut, Universität Bern
Chapter 7: Emissivity measurements, German Aerospace Centre (DLR), Berlin
Chapter 8: Exobiology, Astrobiology Laboratory, Leiden

2. Commonly used soil simulants

The need for good sample materials led to a workshop held at the Lunar and Planetary Institute (Houston, USA) in September 1989 (Conveners: D.S. McKay and J.D. Blacic), where the participants identified some key requirements for the production of large quantities of a *Lunar Soil Simulant*. According to the definition given in McKay and Blacic (1991), a soil simulant is ...:

> "any material manufactured from natural or synthetic terrestrial or meteoritic components for the purpose of simulating one or more physical and/or chemical properties of a (lunar) rock or soil."

Note that this definition of *a soil simulant does not* require to *mimic* many or *all properties* of the simulated soil. This constraint is probably difficult or impossible to overcome, and must be taken into account. If the property to be studied by a specific series of simulation experiments is not representative in a soil simulant "X", then "X" is not a fit soil simulant for the envisaged purpose. Marlow et al. (2008) elaborate on this important aspect in much more detail.

2.1. MSL-1 (lunar)

Weiblen and Gordon (1988) were the first (to our knowledge) to report on the preparation of a lunar soil simulant, called Minnesota lunar simulant #1 (MSL-1). MSL was meant as a lunar mare analogue material, matching the mineralogy, chemistry and texture of the simulated material as closely as possible. In order to achieve a product with a constant and homogeneous quality, the source rock (taken from a quarry in a basalt sill close to Duluth, MN) itself was chosen to be homogeneous, and the manufacturing process followed well documented, reproducible methods, including crushing, grounding and sieving. Though MSL-1 and real lunar mare material (LMM) are chemically quite similar, MSL contains 3.5% ferric iron and 0.4% water, which both are missing in LMM. Furthermore, MSL-1 contains more feldspar and some biotite. While LMM contains glass and mineral agglutinates, both are absent in MSL-1. For more information, see Weiblen and Gordon (1988) and Weiblen et al. (1990). Searching the literature for MSL-1, it appears that this soil simulant has not been used commonly.

2.2. JSC-1 (lunar)

Based on the recommendations and the roadmap given in McKay and Blacic (1991), about 13 tons of a lunar soil simulant were prepared under the coordination of Johnson Space Center. The main characteristics are given in McKay et al. (1993) and, in more detail, in McKay et al. (1994).

The raw material was mined from a basaltic pyroclastic sheet in the San Francisco mountains near Flagstaff, AZ. Compared to other soil simulants that had been produced earlier, JSC-1 is standardized and thus allows direct comparison of results obtained with different techniques and at different laboratories. The aim was to produce a simulant that is chemically, mineralogically and texturally similar to mature lunar mare regolith.

The chemical composition of JSC-1 is somewhat similar to lunar soils at the Apollo 14 landing site, while the grain size distribution better fits coarse lunar soil. A glassy component that is abundant in true lunar soil (''agglutinic glass'') and is produced by micrometeorite impacts is absent in JSC-1 (see Taylor et al., 2004, for instance), though it is relatively glass-rich ($\approx 50\%$). The particle density of JSC-1 ($2.6\,g/cm^3$) is at the lower end of particle densities of lunar regolith ($2.6–3.5\,g/cm^3$). The bulk density of the porous simulant is not given. The mechanical properties (axial strain, principal stresses, elastic constants and density) have been studied by Klosky et al. (1996).

Unfortunately, JSC-1 is no longer available at the prime source, because all samples have been distributed among laboratories around the world.

2.3. JSC-1A, AF and AC (lunar)

After having emptied the JSC-1 stocks completely, there is a need for new sample materials. Carter et al. (2004) suggested the production of large quantities (>100 tons) of a standardized and homogenized baseline or master material, from which several more specialized simulants could be developed, e.g. by implanation of solar wind particles, sieving or admixture of additional components. They point out that a root simulant for lunar highlands would be a desirable option for a second new-generation material.

Meanwhile, JSC-1A lunar mare regolith simulant has been produced to support NASA's future exploration of the lunar surface. The material was created to match, as closely as possible, the composition of the previous JSC-1 lunar regolith simulant. Like the original JSC-1 material, JSC-1A was mined from a volcanic ash deposit located in the San Francisco volcano field near Flagstaff, Arizona. This ash was erupted from vents related to Merriam Crater ($35°20\,N, 111°17'W$), and was collected from a commercial cinder quarry near the south flank of the crater. The mined ash was processed into JSC-1A by ET Simulants, LLC. JSC-1A has a grain size distribution similar to the previous JSC-1 simulant, and is then further processed into JSC-1AF and JSC-AC. The JSC-1AF simulant has a significantly smaller grain size than the previous JSC-1. The average particle size of JSC-1AF is $27.12\,\mu m$, and the median size is $24.04\,\mu m$. JSC-1AC represents a coarser grain size distribution.

A detailed characterization is available at www.lunarmarssimulant.com.

2.4. JSC (Mars-1)

A Mars soil simulant—JSC (Mars-1)—was developed and produced in large quantities since 1997 under the coordination of Johnson Space Center. The raw material was mined on a cinder cone on Hawai'i, Pu'u Nene, which is located close to the saddle road between Mauna Kea and Mauna Loa (see Fig. 1). It was chosen mainly because of its spectral similarity to bright regions on Mars, and consists of weathered volcanic ashes (palagonitic tephra) (Allen et al., 1997, 1998a, b). The chemical composition, mineralogy, spectral characteristics, magnetic properties, volatile content, density and grain size distribution are also given by Allen et al. (1997, 1998a, b). They point out a remarkable difference in density and porosity between JSC (Mars-1) and Martian soil (see Table 2). Both parameters influence quite effectively the thermal and mechanical properties. Therefore, it may not be expected that laboratory measurements using JSC (Mars-1) yield mechanical or thermal properties that are representative for Mars. JSC (Mars-1) contains a significant amount of volatiles, first of all water, while Martian soil is very dry. This difference may influence thermal measurements, exobiology experiments, wind-drift experiments and other measurements.

The particle size distribution of Martian soil, where such data exist, is also different from that of JSC (Mars-1) (see Fig. 2). The heterogenous grain size distribution of Mars-1 causes the material to suffer from segregation—simple agitation causes larger grains to rise toward the surface of a sample. Optical images of the material reveal a degree of non-uniformity among the grains, with darker material being more prevalent at the largest grain sizes. Mars-1 is not processed during its collection or curation so as to remove organic matter. The material should therefore be expected to contain a small amount of organic matter in

Fig. 1. A cinder cone close to the Saddle Road between Mauna Kea and Mauna Loa on Hawai'i. JSC (Mars-1) is produced of material taken from one of these cinder cones (Pu'u Nene) (photo by Ziethe and Seiferlin, 2005).

Table 2
Densities and porosities of JSC (Mars-1), Salten Skov, UK4, Haldit and Martian soil

Source	Allen et al. (1997)	Allen et al. (1998b)	This work
JSC (Mars-1) porosity	54%	–	–
JSC (Mars-1) porosity, after vibration	44%	–	–
JSC (Mars-1) particle density[a]	$1.91 \pm 0.02\,g/cm^3$	–	$2.51\,g/cm^3$
JSC (Mars-1) bulk density	$0.87 \pm 0.02\,g/cm^3$	$0.8\,g/cm^3$	–
JSC (Mars-1) bulk density, after vibration	$1.07 \pm 0.02\,g/cm^3$	$0.9\,g/cm^3$	–
JSC (Mars-1) loose packing	–	–	$0.91\,g/cm^3$
JSC (Mars-1) dense packing	–	–	$0.91\,g/cm^3$
Viking 1 landing site, wind drift	$1.2 \pm 0.2\,g/cm^3$	$1.2 \pm 0.2\,g/cm^3$	–
Viking 1 landing site, blocky soil	$1.6 \pm 0.4\,g/cm^3$	$1.6 \pm 0.4\,g/cm^3$	–
Pathfinder landing site	–	$1.52\,g/cm^3$	–
Viking porosity	$60\% \pm 15\%$	–	–
Salten Skov particle density	–	–	$2.82\,g/cm^3$
Salten Skov loose packing	–	–	$1.20\,g/cm^3$
Salten Skov dense packing	–	–	$1.62\,g/cm^3$
Halditt particle density	–	–	$2.80\,g/cm^3$
Halditloose packing	–	–	$1.09\,g/cm^3$
Halditt dense packing	–	–	$1.52\,g/cm^3$
UK4 particle density	–	–	$2.72\,g/cm^3$
UK4 loose packing	–	–	$1.28\,g/cm^3$
UK4 dense packing	–	–	$1.57\,g/cm^3$

The properties in the last column have been derived from Pycnometer tests.
[a]The derived grain density for the JSC (Mars-1) is considerably higher than in Allen et al. (1997), however, both values are within the limits given by small samples.

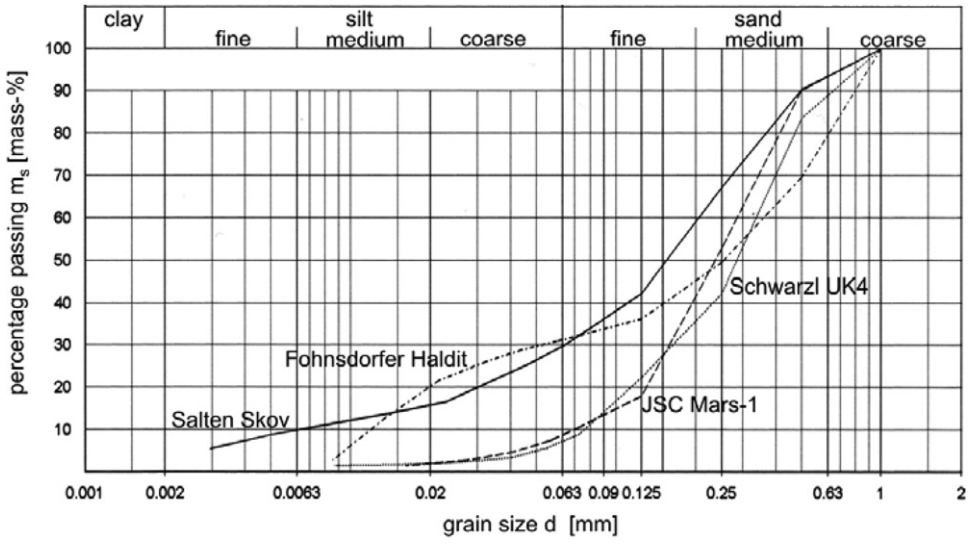

Fig. 2. Grain size distribution of four Martian soil analogue materials.

the form of aerosol deposits, dusts and human effluvia. Some of this bioload will consist of dormant spores of bacteria and fungi (Allen et al., 2000; Mendez et al., 2005) as well as macromolecular compounds associated with their metabolism such as biofilms.

A new type of Martian soil simulant, named *JSC* (*Mars-1A*) was developed very recently and will be available from 30 September 2007. (Refer to www.lunarmarssimulant.com, for details.)

2.5. Salten Skov

Another regolith simulant has been used by European planetary research groups as an analogue for portions of the Martian dust. This dark red soil, hereafter referred to as Salton Skov, is a subsurface deposit from the central Jutland region of Denmark. It occurs over an area of $700\,m^2$ in extent and is rich in precipitates of iron oxides. Salten Skov is meant as a Martian dust simulant and not a

soil simulant. A mineralogical description of this material has been made by Nørnberg et al. (2004). This analogue has had limited use in Martian simulation studies, with emphasis instead placed on its fine grain size and magnetic properties (Merrison et al., 2004). Fig. 2 compares the grain size distribution of Salten Skov with those of other sample materials, incl. JSC (Mars-1). This grain size distribution has been measured on sample material that had been shipped from Aarhus University, Denmark, to Institut für Weltraumforschung, Graz, Austria, and stored for quite some while. The storage and handling caused clodding of small particles in the 2 μm size range. Thus, the size distribution in Fig. 2 does not show the intrinsic size distribution of Salten Skov, which is rather dominated by fine grains in the micrometer range. The silt and clay size fraction (<63 μm) makes up 35.5% of the particles smaller than 2 mm. This fraction was separated from the total sample by dry sieving. It has a free iron content of 35.8% of which nearly 90% is crystalline iron oxides (hematite and maghemite, DCB/oxalate extraction). Most of the grains with a diameter <63 μm consist of aggregates, which can be split into particles 2 μm in size.

The particle size of the <63 μm fraction was determined by laser diffraction and is shown in Fig. 3, taken from Garry et al. (2006) which shows two charts of the same data. The leftmost chart illustrates the complete absence of particles with diameters larger than 0.2 mm. The right-hand side chart in Fig. 3 shows the same data as the left-most chart, but plotted over one tenth of the physical scale, showing that the Salten Skov material is composed predominantly of dust-size particles. No biological assays are available for this material, and in theabsence of contrary evidence it should be expected that this material hosts a bioload of fungal and bacterial spores.

2.6. Other sample materials

In this work we also describe experiments made with sample materials other than those soil simulants mentioned above. Their densities are given in Table 2. For certain kinds of measurements (e.g. thermal and mechanical properties) the grain size, density and shape is more important than the composition. Therefore, other granular materials that are available in large quantities may be a good replacement for "official" soil simulants. Mineral samples used in this work are UK4, Halditt and coarse grained dunite.

UK4 is a mechanical analogue chosen as replacement for the JSC (Mars-1) material from a quarry close to Graz, since for certain penetrometry tests the available amount of JSC (Mars-1) material was insufficient. The name UK4 is the brand name denoting an unwashed sand of maximal grain size 4 mm which was sieved to a maximal grain size of 1 mm for our purpose. The composition is mostly quartz (40%), plagioclase (20%), alkali feldspar (10%), muscovite (15%), hornblende (5%) and dolomite (5%).

Fohnsdorfer Halditt is the weathered excavation residual from the Fohnsdorf (Austria) coal mining site. It was chosen as a mechanical analogue material and has a similar grain size distribution as the Salten Skov material. The composition is mainly quartz (15%), feldspar (both plagioclase and alkali feldspar; ≈20%) and hornblende (10%). Additionally, there are dolomite (5%), iron bearing materials, such as hematite and hydrohematite and sulfate containing materials have been found as traces in the analysis. Also a small amount of muscovite was found in an XRD spectrum.

Small glass beads have been used for thermal measurements—they have the advantage that their size and shape are well defined and the thermal conductivity of glass is well known. Thus the measured data for loose samples can be compared with theoretical predictions based on the properties of the sample.

3. Penetrometry

Penetrometers are usually low speed devices which have been used eg. on the Russian Lunochod or Venera surface units to measure the mechanical properties of the respective surface. This encompasses also the derivation of such

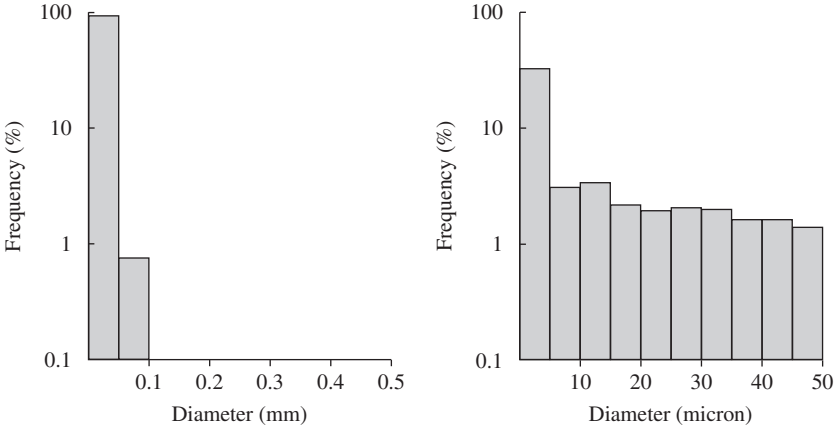

Fig. 3. Size distribution of Salten Skov soil simulant.

properties from mole devices or the measurement of the penetration force of, e.g. the legs of a seismometer, as it was proposed for the Netlander mission. At the upper speed limit of penetrometers are such applications as the Huygens ACC-E penetrometer on Titans surface. To distinguish from low speed aka. static devices for terrestrial applications (e.g. foundation sounding on construction sites) the term quasi-static was introduced, meaning that usually a higher penetration speed is used, but the speed is sufficiently low to still being able to apply static force models.

For the development of a quasi-static penetrometer, a set of soil analogue materials was selected. The requirements for the analogues were twofold, firstly a stable material with easily reproducible properties was needed for the calibration of the instrument and secondly a soil sample representing the Martian surface as close as possible. Thus the selected materials were JSC (Mars-1), Salten Skov and some local materials which were available in larger quantities and having similar mechanical properties as the official Martian analogues. The UK4 material has more or less the same grain size distribution as JSC (Mars-1), and the Halditt is quite close to the Salten Skov material (see Section 2.6). All four soil analogue materials are natural sediments which have been pre-treated prior to their usage. As a calibration standard two types of silica beads with a narrow size distributions were chosen. A list of all materials can be seen in Table 2. It should be noted that our grain density value is larger than reported by Allen et al. (1997). However, since this is a natural material we should expect to have a certain range for the grain densities of small samples excavated from a larger site, i.e. the grain size distribution from spatially separated samples within the same site can be expected to have a variation depending on their exact location within the site.

3.1. Sample characterization

At the beginning of a measurement campaign all of the materials were characterized by applying standard soil-engineering tests. Specifically, the samples had their grain size distributions measured, were exposed to shear- and triaxial-tests, had their grain densities determined and so on. Thus we were able to establish some of the basic soil parameters used for soil models and comparison with the penetrometer measurements (Zöhrer and Kargl, 2006). Mechanical experiments show, that in terms of the grain size all four tested materials were roughly similar to the blocky material found on various landing sites on Mars. The dry bulk density off the tested materials is larger than that of known Martian regolith, even the JSC (Mars-1), which has the lowest density of all sample materials. Estimations of the stiffness for Martian soil (Zöhrer and Kargl, 2006) range from 0.05 up to 2.0 MN/m^2. The Salten Skov has the lowest stiffness of all tested materials with 2.0 MN/m^2 and the UK4 has a stiffness of 4.0 MN/m^2.

It is not possible, with current soil analogues, to match the low modulus values displayed by Mars actual regolith, which in turn suggests that the areas where the Martian rovers sink in more than 10 mm correspond to much finer and thus weaker material. Any comparison between current soil analogues and real Martian regolith may therefore be restricted to either deeper layers where the average grain size is larger, or to only selected areas on the surface.

It should be noted that the preparation and handling of any granular material readily influences its properties, thus making it arduous to achieve similar experimental conditions for subsequent runs or repetitions at other laboratories. Due to segregation and self compaction in samples transported from the preparation site to the experiment, consistent and repeatable sample properties are to achieve only with arduous effort. Thus from the point of view of penetrometry experiments there is no ideal analogue material representing exactly the mechanical or textural properties of, e.g. Mars. For calibration and development of penetrometry experiments, the UK4 turned out to be the most suitable material of all tested species, since it was more stable with respect to clodding and self segregation than all other materials we used thus far. An additional bonus from our point of view was the easy availability in large quantities from a local production site. Silica beads also turned out to be suitable for calibration and modeling as a result of that materials narrow grain size range.

3.2. Penetrometry experiments

For the quasi-static penetrometry experiments a sample was prepared in a cylindrical container with ≈ 260 mm diameter and ≈ 330 mm height. Depending on the exact sensor and tip configuration this allows a typical penetration depth of about 210 mm. In the test rig the penetrometer was driven by a linear actuator with a typical impact speed of some mm/s. The penetration force is measured by two load cells. One is close to the tip of the penetrometer and the other is at the end of the shaft and therefore also sensitive for shaft friction. Typical penetration forces for a granular material can be seen in Fig. 4 and are mainly driven by the sample bulk density. Settling effects in the sample material can be demonstrated by a series of repeated runs into the same sample. Each penetration run is compacting the material and thus resulting in a higher penetration force for each consecutive run (Fig. 5).

4. Aeolian transport of Martian dust

Wind driven grain transport is at present the most active process for modification of the Martian surface, this is due to the widespread transport of dust from the Martian surface into the atmosphere and back again. Although Aeolian sand features are observed many places on Mars detailed study indicates that they are inactive (Greeley et al., 2004). This is contrary to conventional models of

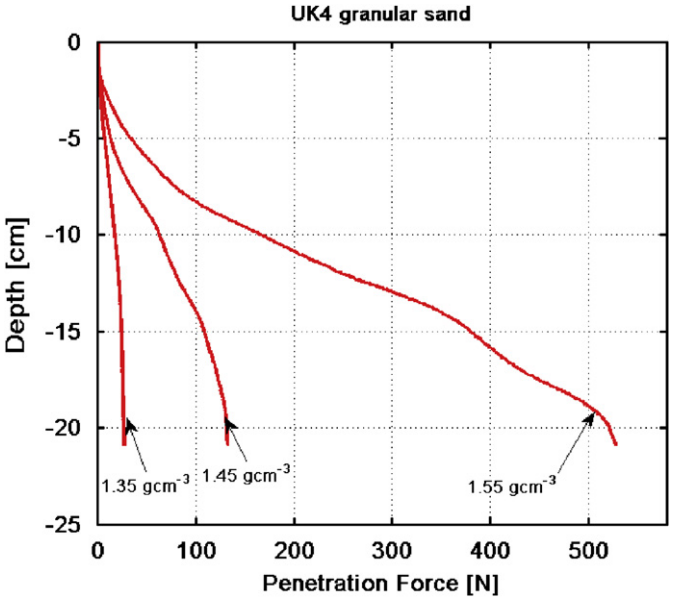

Fig. 4. Typical results from a penetration experiment in UK4 sand.

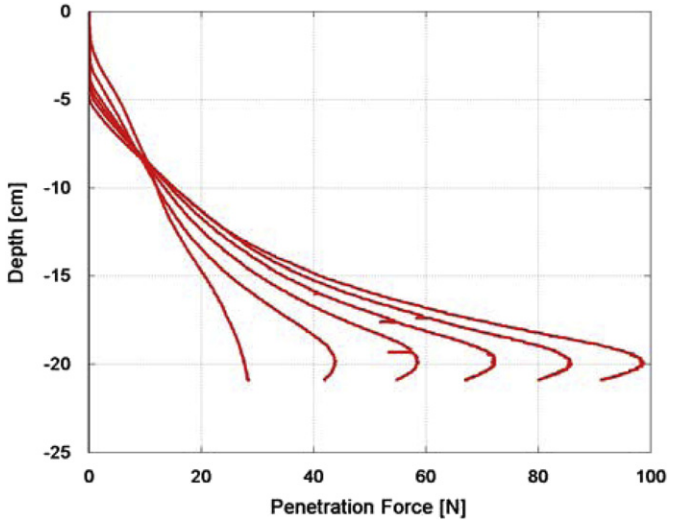

Fig. 5. Material compaction after subsequent runs into the same sample material.

granular entrainment which would predict a lower threshold wind speed for sand sized grains (defined as greater than 60 μm) compared to dust (in this case of a few μm size scale) (Arvidson et al., 2004). Note that generally dust can be suspended in the atmosphere whereas sand grains cannot. At present the most likely transport mechanism for Martian dust involves the formation of (electrostatically bound) sand sized aggregates which have a low effective mass density and therefore have a significantly reduced entrainment threshold wind speed. Aggregate breakup then results in re-suspension of electrified dust grains (Greeley, 1979; Merrison et al., 2004). Though supported by observations in earth based simulations there is only indirect evidence for this process from Mars. Dust aggregation is supported by, for example, analysis of MER magnetic properties experiments and microscopic/camera observations (Herkenhoff et al., 2004; Kinch et al., 2006). If correct this dust transport mechanism would imply that the grain size of Martian dust (bright surface material) is a dynamic and broadly distributed parameter.

There are two substantial experimental investigations of granular transport under Martian simulated conditions, the first being in the NASA Ames MARSWIT wind tunnel facility and more recently studies at the Aarhus Mars Wind tunnel facility (Greeley and Iversen, 1985; Merrison et al., 2002). The former uses an open circuit flow and is best suited to high wind speeds (at low pressure) and has been used to quantify sand saltation threshold. The latter is a re-circulating system and has concentrated mostly on dust transport. In both cases analogue dust injection into the wind flow has been achieved by allowing a mixture of dust and gas (air) to be drawn into the wind tunnel. Here dust aggregates are dispersed in the turbulent flow. For such earth based Martian dust analogue materials grain size is crucial when studying wind induced transport. Reproducing the fine (few micron) suspended dust fraction observed in the Martian atmosphere is of great importance. In such studies significant adhesion and cohesion of dust is observed and a large degree of dust electrification (Greeley et al., 2000; Merrison et al., 2002, 2004). Although detailed studies of the dependence of such behavior on mineralogy are still to be performed, preliminary investigations suggest that there is not a strong dependence on material mineralogy.

Salten soil was initially chosen as a Mars simulant because of its magnetic properties, which have reproduced most of the observations of the (several) magnetic properties experiments performed on Mars to date (Kinch et al., 2006). This analogue is, however, also extremely fine grained and homogenous (from sample to sample) when dispersed. It is this feature which has made it well suited for simulation of the Martian dust aerosol. Specifically it has been used extensively for studying dust magnetic properties, dust electrification, dust deposition, removal and adhesion as well as testing, developing and calibrating instrumentation (Kinch et al., 2006; Merrison et al., 2002, 2004; Gunnlaugsson et al., 2005). Salten analogue grains injected into the Aarhus wind tunnel have been measured to have a mean diameter of around 2 μm (Merrison et al., 2002), in reasonable agreement with Martian dust of around 3 μm. Though the material has a bulk density of around 3000 kg/m^3 the powder is generally loosely packed with a density around 1000 kg/m^3. Single aggregate grains have been observed to have even lower density, as low as 400 kg/m^3. Other dust materials (not widely utilized as Mars simulants) have been used in wind tunnel simulations for studies of dust transport. One example is Rivendale red clay (Greeley et al., 2000), which is also available in large quantities and is fine grained. Also pure iron oxide minerals, for example hematite and magnetite, have been used for specific studies (Merrison et al., 2002; Kinch et al., 2006. Most recently it has been proposed to

develop powdered basalt as Mars dust analogue; this is based on observations by the MER of the mineralogy of the Martian dust (Gunnlaugsson et al., 2005). JSC (Mars-1) and other Hawaiian palagonite materials, though containing a fine grained fraction, also contain a large fraction of larger solid grains (sand sized) and show variability from sample to sample. They may therefore be a good analogue for a mixed sand and dust soil, though they are not ideal for studying wind transport of Martian dust or sand.

In Aeolian transport studies the lower Martian gravity has been re-produced by using low mass density materials such as walnut shells, silica gel, instant tea (Greeley and Iversen, 1985) and carbon powder. More recently, however, studies have used commercially available hollow glass spheres. Here the surface morphology and adhesive properties can be maintained while varying the effective mass density (or gravity). In this way it is also possible to simulate the reduced mass density of dust aggregates. These studies have reproduced the observation of reduced detachment threshold wind speed for dust with respect to sand grains. The process of dust aggregate breakup is, however, not reproduced and remains to be studied in detail (Fig 6).

To conclude it should be said that with regard to wind transport there remains a large number of possible Mars dust and sand analogues, with varying properties depending on the experimental conditions. In large part this is due to a lack of observational constraints from Mars and it is only through new and improved direct measurements of wind induced grain transport from Mars that analogue materials will improve. Specifically measurement of (local) wind speeds/turbulence related to observation of granular transport is necessary. Crucial parameters to be measured with respect to dust include the size (distribution), dust electrification and direct determination of the dust concentration and its variation. For sand sized (solid) grains the threshold wind speed for detachment should be quantified, the effects of induration should be studied and extensive age determination made of sand transport features.

5. Thermal conductivity

In order to understand whether or not soil simulants are good sample materials for thermal conductivity measurements, it is important to be familiar with heat transport in porous media. Therefore, we start this section with a brief overview of this subject.

5.1. Heat conduction in porous media

While for bulk materials the thermal conductivity is a material property that, once determined, can be taken from tabulated values, this is not the case when porous materials are considered. For soils and regoliths, porous ice and ice–dust mixtures, the mineralogical composition of the solid part of the medium has a minor effect, since the bulk thermal conductivity for most minerals and water ice differ by only about a factor of two, while other properties of the sample can have a much larger effect. The solid-state conductivity of the matrix depends on the microstructure of the matrix, i.e. the availability and distribution of direct connections between solid particles in the direction of the considered heat flow. The total cross section of solids compared to voids in a given layer is reduced compared to a void-free material, and acts as a bottle neck for conduction. When only soil and regolith type materials are considered, the contact area between single grains is the most important single parameter. Cementation, interstitial ice and sintering (applicable for porous ice) can substantially increase the thermal conductivity, while the porosity and overall density is almost unaffected, because only very little material is needed to increase the cross section of bonds at the contact point between adjacent grains. In the relevant literature it is not uncommon to regard the porosity of a medium as the key parameter, and empiric observations or measurements seem to support this approach. However, in most of these cases the samples are simply compressed in order to increase their density and decrease their porosity. Compression also increases the contact area, which is the true reason for the observed effect. A good overview of the thermal conductivity of

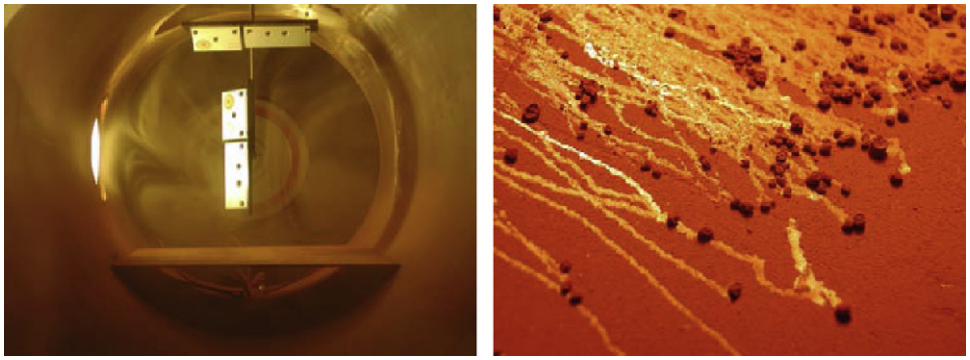

Fig. 6. On the left a photograph shows a view inside the Aarhus wind tunnel while exposing Pathfinder magnets to suspended Martian dust analogue. On the right a photograph taken inside the wind tunnel illustrating dust aggregates forming which become so large (several mm in diameter) that they are able to roll.

consolidated (e.g. cemented or sintered) and unconsolidated (i.e. loose) materials can be found in Presley and Christensen (1997a, b, 2006). The effect of sintering on the thermal conductivity of comets is studied in Seiferlin et al. (1995). Artificially cemented samples have been investigated by Seiferlin et al. (2007).

When the pores are filled with gas, the overall heat transport is no longer provided by the matrix alone. The contribution of the gas to heat transport is provided by two fundamentally different processes: (a) heat is carried as the averaged kinetic energy of gas molecules, and is exchanged with the matrix by collisions, and (b) sublimation of volatiles such as water or CO_2 ice in warm regions and recondensation in cold regions carries latent heat between the two regions where phase transitions occur. The community of thermophysical comet modellers and their publications are a good source for a theoretical description of heat transport by gas in a porous medium (see Benkhoff and Spohn, 1991; Steiner and Kömle, 1991, for example). The latent heat effect (b) can be neglected for the Moon and other warm and dry places in the solar system. For Mars, (b) might be important when the Martian polar caps and the ice-rich regions at high latitudes are considered. For both contributions, (a) and (b), the ambient pressure and the size of the pores play a major role. If the mean freepath at a given pressure is larger than the pore size, every single gas molecule can carry heat directly from the cold side of the pore to the warm side. Therefore, the overall heat flux increases with pore size and with pressure. If the mean free path is smaller than the pore size, gas molecules collide with each other and exchange heat. The surplus of gas molecules does not contribute to the overall heat flux, because the same "heat package" is handed over from molecule to molecule before it finally reaches the cold pore face. Increasing the pore size or increasing the pressure both have no influence on the heat flux any more, and the measured effective thermal conductivity is constant with respect to pressure changes. Note that this is in particular true for heat conduction in air, because the atmosphere may be seen as an infinitely large pore. Obviously, a measured value for the thermal conductivity of a porous sample that is filled with gas depends strongly on the ambient pressure *inside* the pores, and the pore size. While the pore pressure in soil can vary with time and depth, the pore size is typically not uniform; it rather follows the grain size distribution of the matrix, which in turn may also be a function of depth.

5.2. Sample materials for thermal conductivity measurements

Measurements with soil analogues—whether standardized products or sand, terrestrial soils and ices—are ultimately desirable, but the results will always be heuristic and cannot easily be compared to theoretical derivations or models. The thermal conductivity depends on sample characteristics such as pore size distribution and degree of cementation, layering in the sample and other inhomogeneities, and moisture and interstitial ice, as we have seen in Section 5.1. The abundance and spatial distribution of H_2O in both liquid and solid form is furthermore variable with time, last not least because of the evacuation of the sample at the beginning of a measurement campaign. It is not easy to dessicate a fine-grained material with a very large specific surface before the sample can be used in the vacuum chamber. In addition to these uncertainties, there might be practical problems like those discussed in Section 5.3. On the other hand, the sample parameters that standard soil simulants like JSC (Mars-1) try to mimic, e.g. composition and color, have no or very minor influence on the thermal conductivity. Therefore, we prefer to use artificial samples that are easy to handle and well known with respect to their pore size, grain shape, degree of cementation, volatile content (including water) and spatial homogeneity. A systematic variation of one or more of these key parameters allows one to derive or evaluate theoretical descriptions or models of their thermal conductivity.

5.3. The thermal conductivity of JSC (Mars-1)

Regardless of the problems with realistic sample materials like soil simulants, we made the attempt to measure the thermal conductivity of JSC-1 (Mars) at pressures around 5 mbar, i.e. a pressure that is typical for Mars. We applied the *line heat source* (LHS) technique, also known as the *transient heated wire* method. The technique is for good reasons very popular and well-suited for the conditions (temperature, pressure, thermal conductivity and sample characteristics) we have to deal with. We (K. Seiferlin, Universität Bern, and G. Kargl, N. Kömle, Institut für Weltraumforschung, Graz) applied this technique already successfully with porous water and CO_2 ice samples in vacuum (Seiferlin et al., 1996; Banaszkiewicz et al., 1997). A detailed description of the method, including theory and data evaluation, is also given in Seiferlin et al. (1996). The JSC (Mars-1) soil samples have been dried in a pot on an oven until no vapor condensed on a cold surface held above the pot. It was then filled into a sample container of about 12 cm diameter and 15 cm height. The sample container was covered by a lid, and finally the LHS thermal conductivity sensor was inserted through a hole in the lid into the sample. The sample container was then placed into a vacuum chamber that is equipped with an oil diffusion pump. During evacuation the pore-filling gas cannot leave the sample easily because the gas diffusion coefficient of the sample material is small. Consequently, a pressure gradient between the chamber and the sample builds up. To our surprise the gas drag from the sample was powerful enough to lift dust particles from the sample and carry them through the hole in the lid. Most of the dust grains sedimented on the lid (see Fig. 7), but the finest dust particles made it into the oil of the pump, and seriously damaged it. When similar measurements are to

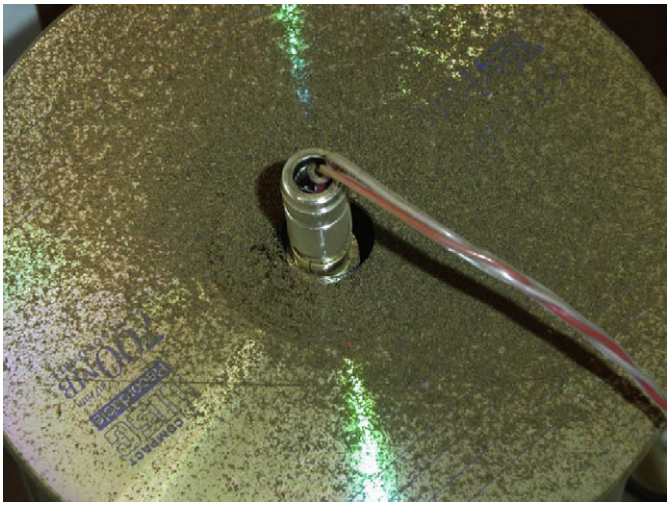

Fig. 7. JSC (Mars-1) soil simulant, ejected from a sample below a CD-ROM (used as lid) during chamber evacuation due to overpressure within the sample, dragged by gas through the central CD hole and deposited on the CD. The cable and connector of the thermal conductivity sensor can be seen at the CD hole.

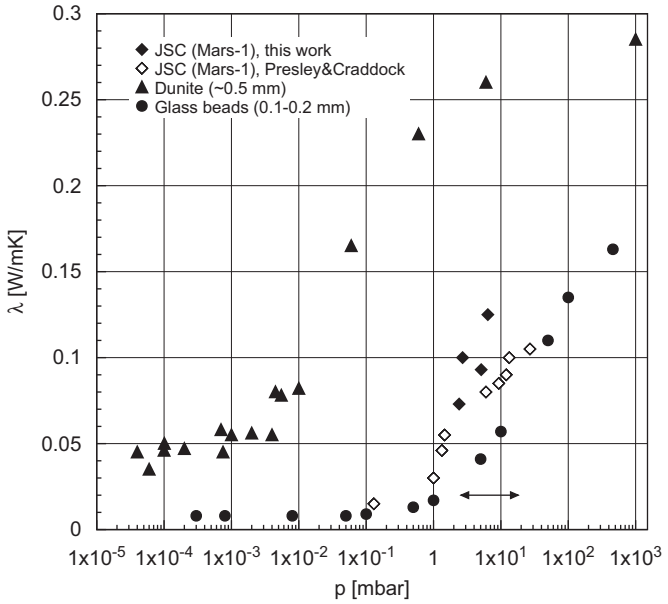

Fig. 8. Thermal conductivity of JSC (Mars-1) soil simulant (this work: filled diamonds; Presley and Craddock (2006b): open diamonds), coarse-grained dunite (black triangles) and glass beads (filled circles) of ≈ 0.15 mm diameter at various pressures. The pressure range on Mars is indicated by the arrow.

be performed in the future or by other groups, precautions should be taken to protect the chamber and the pump against damage, and the pressure reduction by pumping should be at a rate slow enough to prevent large pressure gradients between the sample and the chamber.

The damage of the pump forced us to stop the campaign after only a few measurements, of which some suffered from not yet stable pressure inside the voids of the sample. It is a convenient side effect of the LHS technique to reveal any violations of ideal conditions by a non-linear transient temperature increase vs. a log time scale. Since pressure influences the thermal conductivity and the pressure inside the sample pores decreased during some transient measurements runs, such runs can easily be identified and sorted out. A total of merely four good measurements remained (see Fig. 8). It is somewhat questionable to interpret a data set of only four points, and we are very cautious to do so, but progress in science is based not only on success but also on failure, and therefore we want share the experience. The measured thermal conductivity compares well with measurements made by Presley and Craddock (2006b). The remaining differences between our work and that of Presley and Craddock (2006b) can be attributes to differences in the sample, e.g. grain size distribution, sorting, sample preparation and settling, humidity, etc.

It should be noted that, as explained in Section 5.1, the effective thermal conductivity depends on the actual grain size distribution compared to the mean free path of the gas molecules, which scales with pressure. For lower pressure, lower thermal conductivity values are to be expected, while for large pressures a constant but comparatively high thermal conductivity would be observed. The general trend in Fig. 8 is therefore in agreement with theory (see Presley and Christensen, 1997a, b, 2006, for example).

For comparison, a data set measured with a coarse-grained dunite sample (≈ 0.5 mm grain size) and measurements of glass beads with ≈ 0.15 mm diameter are shown (see Seiferlin et al., 1996 for a detailed description of the dunite data set). The transition between low and high thermal conductivity values occurs at a pressure that depends on the actual pore size (see Section 5.1), and the transition pressure is lower for large pores. This is, again, consistent with the results: for the fine-grained JSC (Mars-1) the transition occurs just in the pressure range that is relevant for Mars (5–10 mbar), while for the coarse dunite sample the transition occurs at much lower pressure (10^{-2}–1 mbar). Note that the Martian atmosphere shows a significant variation in pressure, both with time and location. Because the thermal conductivity of Martian soil is not pressure-independent but is rather a function of both pore size distribution and pore pressure, the actual thermal conductivity of Martian soil will vary with location and ambient conditions.

In addition to the more general disadvantages of using "realistic" soil simulants discussed above, the practical problems encountered in our measurement campaign must be taken into account when planning similar studies.

6. Bidirectional reflectance

Bidirectional reflectance is a photometric quantity which characterizes the fraction of light that an illuminated surface scatters into a given direction per unit solid angle. It is dependent upon the illumination and observation geometry as well as the physical properties of the light scattering medium. As spectral studies of a regolith can be

used to identify the presence of specific minerals via the detection of absorption bands that are characteristic of those minerals, bidirectional reflectance distribution function (BRDF) studies of a regolith can provide insights into the small-scale regolith structures that fall within a resolution element of an imaging data set. These structures might include properties such as grain size/shape distributions or regolith porosity. For example, the BRDF of planetary surfaces is commonly stronger back in the direction of the illumination source (i.e. at near-zero phase angles) than towards higher phase angles. These reflectance features, known as an opposition surges, are often attributed to the disappearance of small scale shadows as the observer approaches zero phase angle. Fig. 9 demonstrates laboratory-based opposition surge measurements in four optical bandpasses. The width and magnitude of the opposition surge cusps tend to be higher for fluffier soils. Reflectance models, such as the commonly used models of Hapke (1993), can be used to quantify these small scale properties. However, the models cannot treat an unlimited variety of surface conditions explicitly. To prepare for the interpretation of some hypothetical surface configurations and validate the model modifications that are necessary to describe those configurations, laboratory data are important. For example, Johnson et al. (2004) measured the BRDFs of dust coated rocks and evaluated their ability to determine dust layer thicknesses on Martian rocks remotely. Gunderson et al. (2006) measured the BRDFs of dry and wet samples to assess the possibility of identifying potentially wet localized surface regions on the Martian surface using visible/NIR imaging data. Since actual samples of the Martian regolith are not available, regolith simulant must be used for these types of studies. A common choice is JSC (Mars-1) (Allen et al., 1997). As shown in Fig. 10, JSC (Mars-1) simulant is spectrally similar to true Martian regolith, and is believed to be mineralogically similar.

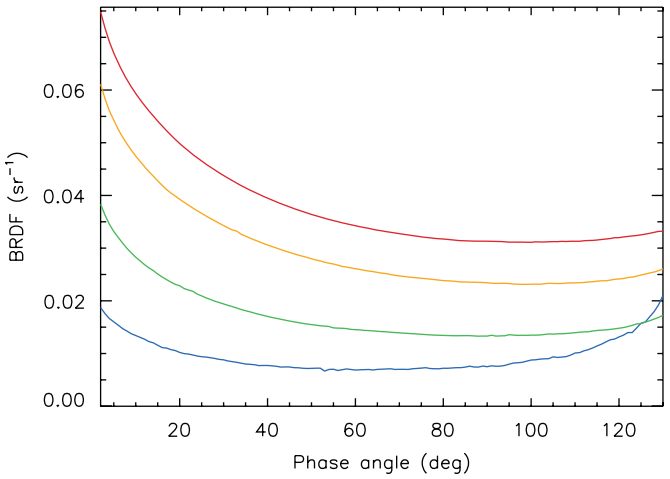

Fig. 9. BRDFs of JSC (Mars-1) regolith simulant in four optical bandpasses with characteristic wavelengths of 462 nm (blue), 558 nm (green), 672 nm (orange) and 875 nm (red).

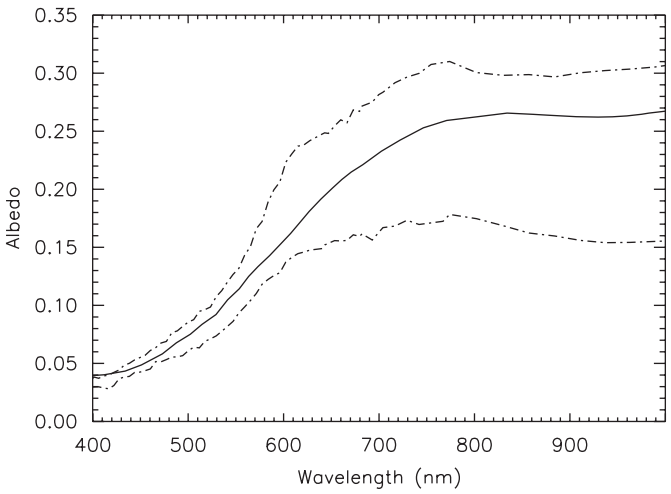

Fig. 10. Solid: Reflectance spectrum of JSC (Mars–1) regolith simulant (Allen et al., 1997). Dash-dot: Typical spectra of bright and dark regions of Mars (Mustard and Bell, 1994).

7. Emissivity measurements

Emission spectroscopy of planetary surfaces is one of the most powerful tools for the investigation of surfaces composition. Nearly every current mission to Mars has on board an instrument devoted to such kind of studies. Some actual examples are the Thermal Emission Spectrometer (TES) on Mars Global Surveyor (Christensen et al., 2001), the imaging spectrometer THEMIS on Mars Odyssey (Christensen et al., 2003) and the Planetary Fourier Spectrometer (PFS) onboard Mars Express (Formisano et al., 2005). Furthermore, a new generation of instruments is being developed, such as the thermal infrared imaging spectrometer MERTIS on the ESA Bepi-Colombo mission to Mercury, that will map the whole planet with a spatial resolution of 500 m and a spectral resolution of up to 90 nm in the wavelengths range from 7 to 14 μm (Helbert et al., 2005). The emission spectra of planetary surfaces contain extensive information about mineralogical composition and surface properties, although, to extract reliable compositional information from the remote sensing spectra, it is necessary to study the spectral behavior of analogue materials using laboratory spectroscopic measurements. Composition and structure and other physical/textural properties of the material, including grain size distribution, surface roughness, packing density, crystallinity and preferential orientation of crystals, affect the band shapes and depths. The Berlin Emissivity Database (BED) is a spectral database of particle sizes separates in the range from <25 μm to 250 μm, measured at 90 C and atmospheric pressure in the wavelength range from 6.3 to 22 μm. The spectral measurements are performed with a Fourier transform infrared spectrometer (Bruker IFS 88), purged with dry air and equipped with a liquid-nitrogen-cooled HgCdTe (MCT) detector, coupled to the emissivity device built at DLR (Berlin). All spectra are acquired with a spectral

resolution of 4 cm^{-1}. Further details on the instrument, measuring rationale and emissivity calculation can be found in Maturilli et al. (2006, 2008). The BED spectral library contains spectra of plagioclase and alkali feldspars, pyroxenes, clays, olivines, quartz, sulphates and others. Four particle sizes has been selected to better represent the planetary soil conditions: 0–25, 25–63, 63–125 and 125–250 μm.

Fig. 11 shows the emission spectra of palagonite from Pahala Ash, Hawaii, USA. Palagonite is the product of vetrification of basalt at low temperatures, and is commonly considered as a Martian soil analogue. In fact, the JSC (Mars-1) is actually a palagonitic tephra coming from the Pu'u Nene cinder cone on the island of Hawai'i, USA. The spectral feature at 1150 cm^{-1} (or around 8.7 μm), is the highly diagnostic Christiansen maximum or feature (CF), a maximum in emissivity whose position is unaffected by particle size, at 1 bar pressure. The feature at about 1050 cm^{-1} (or 9.5 μm) in Fig. 11 is the mineral's Reststrahlen band, caused by the strong stretching of the Si–O bonds. The positions and shapes of Reststrahlen bands are specific for the respective material, although the shapes are strongly affected by particle size and crystal orientation. For the two size separates where small particles are dominant (<25 and 25–63 μm) the contribution of volume scattering is significant. For these small particles, the spectral contrast within the Reststrahlen band is strongly reduced and a separate emission minimum is evident at about 870 cm^{-1} (11.5 μm). The extreme differences between the spectra of coarse-grained and fine-grained separates are caused by the growing influence of volume scattering with decreasing particle size. To note the two large adsorption bands in Fig. 11 centered around 1330 cm^{-1} (7.6 μm) and 1570 cm^{-1} (6.35 μm). The center of the large adsorption band between 1200 and 1400 cm^{-1} is found at the same position for the smaller grain sizes, while it shifts and decreases considerably for the larger grain sizes. The shape and depth of the adsorption band between 1500 and 1650 cm^{-1} changes dramatically with the grain size range, while the center remains constant. The small bands between 1400 and 1600 $cm^{-1}$and the large band centered around 667 cm^{-1} are due to remnant water vapor and CO_2 in the emissivity chamber.

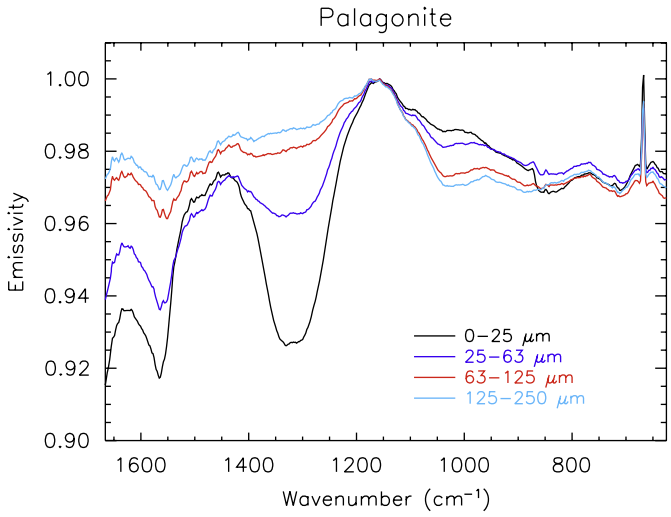

Fig. 11. Emission spectra of palagonite separates.

8. Exobiology: survival of organics in simulated planetary environments

The detection of residual organic compounds that might be present from either biotic or abiotic sources on the Martian surface and subsurface is among the main goals of future Mars missions. The Viking spacecraft did not find any trace of organic matter on the Martian surface above the detection limit of the landers payloads. Given the probable input of meteoritic organic compounds to the Martian surface, the absence of such compounds may have been caused by environmental alteration of organic material on and in the Martian surface due to energetic radiation, dryness and oxidization (Banin, 2005; Zent and McKay, 1994). Organic matter, including that delivered from extra-Martian sources, would have suffered multiple poorly understood weathering processes, including gardening of the surface dust, UV photolysis and mineral-catalyzed oxidation reactions.

Laboratory simulations provide a convenient path for the understanding of chemical reactions on the Martian surface. We have studied the behavior of organic matter under simulated Martian conditions by using small atmospheric simulation chambers in combination with deuterium and xenon lamps. We have recently shown that pure amino acids films can be destroyed by exposure to UV light with a spectrum similar to that found at the surface of Mars, and the rate of degradation is high relative to geological timescales (Ten Kate et al., 2005) unshielded glycine and D-alanine molecules exposed directly on the Martian surface have half-lives of the order of 10^4-10^5 s under noon-time conditions at the Martian equator (see Fig. 12). More complex molecules are expected to be altered either by photolytic or photochemical pathways (Quinn et al., 2005).

Peeters et al. (2008) recently measured the pH, redox potential, ion concentrations, as well as carbon and amino acid abundances of Mars analogue soils from the Atacama desert. The results indicated that the surrounding mineral matrix is a key to understanding the survival of organics on Mars. Variations in chemical and physical properties, water abundance, UV exposure and other variables have profound effects on measured decomposition rates in laboratory simulations (Peeters et al., 2008).

In order to simulate realistic planetary conditions the behavior of organic molecules has to be tested in appropriate Martian soil analogues. The effect of mineral surfaces on the degradation processes associated with organic matter exposed at the surface of Mars has been investigated by several groups (Oró and Holzer, 1979;

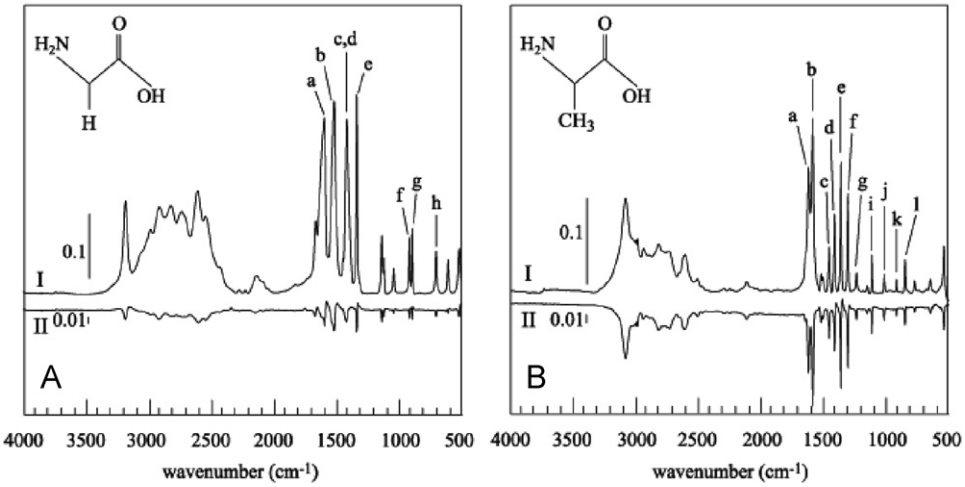

Fig. 12. The infrared spectrum of (A) solid glycene and (B) solid D-alanine in the range 4000–500 cm^{-1} measured with a resolution of 4 cm^{-1}. Two spectra are shown, (I) is recorded before irradiation with a deuterium discharge lamp, and (II) is obtained by subtracting the spectrum of the unirradiated compound from the spectrum recorded after 50 h of irradiation (taken from Ten Kate et al., 2005).

Huguenin et al., 1979; Stoker and Bullock, 1997; Yen et al., 2000). The introduction of any mineral component raises the complexity of an experiment dramatically when compared to simple irradiation studies of thin films. Identification of the significant organic contaminant make-up of existing regolith standards, such as JSC (Mars-1) (Allen et al., 1998b) from the Johnson Space Center, is a necessary step when such materials are used as analogues for Martian surfaces. With no prior cleaning, two commonly available regolith analogues have been shown to interfere with studies of the response of organic matter to the Martian environment. Any terrestrial soils are extensively contaminated with extant biota. We characterized the amino acid content of simulants with high-performance liquid chromatography and showed the presence of over a dozen amino acids with average concentrations of 10 ppm (Garry et al., 2006), see Fig. 13. Such contamination is in-line with other studies which have demonstrated the presence of bacterial spores in the Mars-1 analogue (Mendez et al., 2005).

Our results also indicated that monolayers of water (representative of Martian equatorial regions; Möhlmann, 2004) that were adsorbed on soil samples effectively enhanced the degradation of amino acids in Martian soil analogues (JSC (Mars-1)) when exposed to simulated Martian UV lighting conditions (Garry et al., 2006). Experimental studies with single-component minerals have emphasized the role that adsorbed water can play, and it is possible that the presence of quasi-liquid films of water is critical to the formation of oxidizing agents. The low but non-zero humidity of the Martian atmosphere implies that water will be present on surfaces in diffusive contact with that gas. If water adsorbed onto a mineral grain can leach soluble species from the rock, then the photo-Fenton reaction (abbreviated from Walling, 1975) can occur, namely

$$H_2O_2 + Fe^{3+}_{aq} = Fe^{2+}_{aq} + HO_2^- \cdot + H^+$$

This process is well known on Earth Southworth and Voelker (2003) and has been postulated as an explanation for the rapid destruction by oxidation of organic species (Benner et al., 2000; Möhlmann, 2004). The perhydroxyl radical formed from this reaction is more vigorous than the hydroxyl radical which is commonly used to degrade organic matter in industrial processes. Clearly, the process is limited at the surface of Mars by the availability of hydrogen peroxide and aqueous iron salts. At first glance such a scenario is unlikely for the desiccated surface of Mars in the current epoch. However, quasi-liquid films of unfrozen water can persist on mineral grains cooled to temperatures comparable to those found on Mars, with the film thickness governed by the ambient humidity. The amount of water vapor needed to produce a monolayer of water at the conditions found at surface of Mars is not large; the Martian surface partial water vapor pressure of around 10^{-3} mbar is used in a theoretical model presented by Möhlmann (2004) to predict that an equilibrium state of a few (≈ 5) monolayers of water would be ubiquitous on exposed Martian surfaces. This quasi-liquid water layer would vary in thickness throughout the Martian year, waxing and waning with the temperature and water vapor partial pressure of the local atmosphere.

The survivability of organic matter when exposed to hostile conditions on the surface of planetary bodies is critical for preserving biosignatures of life. Moreover, these processes are also important in determining the fate of organic material that was delivered to early planetary bodies, including early Mars and Earth. Laboratory simulations using soil analogues as well as field tests in the Atacama desert have shown that the interaction of radicals, adsorbed water and mineral soils play an important role in the destruction of organic material on the Martian surface (Quinn et al., 2005). Recent results also demonstrated that organic molecules and their degradation products are well preserved in sulfate minerals on Earth

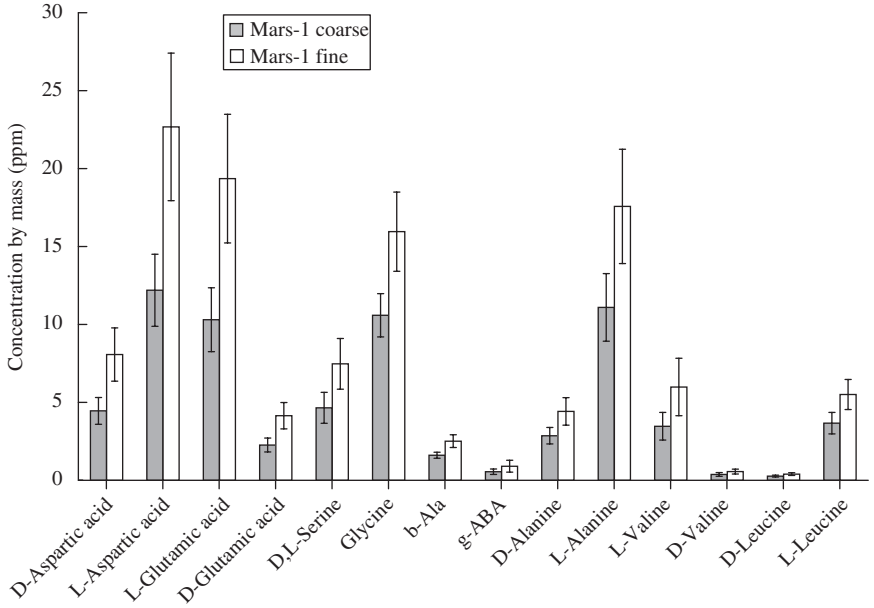

Fig. 13. Average absolute blank-corrected amino acid concentration in the unirradiated samples of coarse and fine-grained fractions of JSC (Mars-1) (taken from Garry et al., 2006).

(Aubrey et al., 2006). Results from the MER rovers indicate the presence of sulphate minerals and further studies using different Martian analogues appear to be excellent simulations to support the search for organic compounds on Mars during future missions. Monitoring the evolution of organic matter as it is exposed to present and past Martian conditions will provide important limits to exobiological models, support current and planned space missions and address issues of planetary protection.

9. Summary

The experimental work and the facilities used which are described in this paper represent most probably only a fraction of groups that have worked with soil simulants. Nevertheless, the measurements we describe in Sections 3–8 cover a wide range, from mechanical and thermal through optical properties and up until chemical and biological studies. In all of these examples there are a few considerations to be made that can be—and often are—easily be forgotten: the results apply for the studied samples which are all terrestrial, and it remains unclear how far the results can be transferred to true extraterrestrial material under relevant conditions. While returned samples are unavailable in such quantities that they could be regarded as disposable, this situation will not change, and this appears to be the case in the near-term future. Even returned samples would not always improve the situation, because sampling and transport may change the properties in question, and the ambient condition in the laboratory might not be close enough to those at the sampling site (see Section 5 for a more detailed discussion). Certain mineralogical or physical aspects might be not properly mimicked by any of the available soil simulants. We have seen, for example, that especially for the "physical" measurements the actual mineral composition is rather unimportant while the density, grain size and shape are very important. The commonly used soil simulants aim at mimicking the former and to less extent the latter. In such cases, artificial samples with well-known properties might be a better choice, because uncertainties about clodding, grain and pore size and shape, composition, etc. can be controlled in a systematic way.

The gap between laboratory measurements on analogues on one hand and the behavior of real soils on the other hand can only be closed by scientific instruments flown as part of the payload of future missions. While the measurements of optical properties, as described in Sections 6 and 7 can help understanding remote sensing data, the experiments described in the remaining sections address landers, rovers and surface stations. *In situ* measurements must be compared to more systematic and extensive laboratory measurements in order to understand both. The European ExoMars rover is planned to carry several instruments (e.g. Corbel et al., 2006; Federico et al., 2007; Griffiths et al., 2006; Hamelin et al., 2006; Marzo et al., 2006; Parnell et al., 2007; Patel et al., 2006; The Rover Team et al., 2006; Ulamec et al., 2006; Vago et al., 2006, 2007) which would profit from accompanying laboratory work. ExoMars will also deliver a small geophysical surface station called GEP (Spohn et al., 2006; Biele et al., 2007) which houses instruments that address mechanical and thermal properties (Spohn et al., 2001a, b; Richter et al., 2003; Wieczorek et al., 2007). The continuation of measurements in different disciplines, performed by a collaborating network of laboratories, can support the development of *in situ* instrumentation

and, at the same time, will build up expertise to plan, perform and evaluate *in situ* measurements.

Acknowledgments

We wish to thank Marty Gustafson from *orbitec* (http://www.lunarmarssimulant.com) who provided early information about the next generation soil simulants, JSC (Mars-1A) and JSC-1A, -1AF and -1AC (Lunar). Vincent F Chevrier and one unknown referee helped to improve the paper significantly by providing comprehensive reviews to the first manuscript.

References

Allen, C.C., Morris, R.V., Lindstrom, D.J., Lindstrom, M.M., Lockwood, J.P., 1997. JSC Mars-1: Martian regolith simulant. In: Lunar and Planetary Institute Conference Abstracts, March, p. 27–+.

Allen, C.C., Jager, K.M., Morris, R.V., Lindstrom, D.J., Lindstrom, M.M., Lockwood, J.P., 1998a. JSC Mars-1: a Martian soil simulant. In: Galloway, R.G., Lokaj, S. (Eds.), Space, vol. 98, p. 469–+.

Allen, C.C., Morris, R.V., Jager, K.M., Golden, D.C., Lindstrom, D.J., Lindstrom, M.M., Lockwood, J.P., 1998b. Martian Regolith Simulant JSC Mars-1. In: Lunar and Planetary Institute Conference Abstracts, March, p. 1690–+.

Allen, C.C., Griffin, C., Steele, A., Wainwright, N., Stansbery, E., 2000. Microbial life in Martian regolith simulant JSC Mars-1. In: Lunar and Planetary Institute Conference Abstracts, March, p. 1287–+.

Arvidson, R.E., Anderson, R.C., Bartlett, P., Bell, J.F., Blaney, D., Christensen, P.R., Chu, P., Crumpler, L., Davis, K., Ehlmann, B.L., Fergason, R., Golombek, M.P., Gorevan, S., Grant, J.A., Greeley, R., Guinness, E.A., Haldemann, A.F.C., Herkenhoff, K., Johnson, J., Landis, G., Li, R., Lindemann, R., McSween, H., Ming, D.W., Myrick, T., Richter, L., Seelos, F.P., Squyres, S.W., Sullivan, R.J., Wang, A., Wilson, J., 2004. Localization and physical properties experiments conducted by spirit at Gusev srater. Science 305, 821–824.

Aubrey, J., Cleaves, J., Chalmers, J., Skelley, A., Mathies, R., Grunthaner, F.J., Ehrenfreund, P., Bada, J.L., 2006. Sulfate mineral and the search for organic compounds on Mars. Geology 34 (5), 357–360.

Banaszkiewicz, M., Seiferlin, K., Spohn, T., Kömle, N.I., 1997. A new method for the determination of thermal conductivity and thermal diffusivity from linear heat source measurements. Rev. Sci. Instrum. 68 (11), 4184–4190.

Banin, A., 2005. The enigma of martian soil. Science 309, 888–890.

Bell, J.F., McSween, H.Y., Crisp, J.A., Morris, R.V., Murchie, S.L., Bridges, N.T., Johnson, J.R., Britt, D.T., Golombek, M.P., Moore, H.J., Ghosh, A., Bishop, J.L., Anderson, R.C., Brückner, J., Economou, T., Greenwood, J.P., Gunnlaugsson, H.P., Hargraves, R.M., Hviid, S., Knudsen, J.M., Madsen, M.B., Reid, R., Rieder, R., Soderblom, L., 2000. Mineralogic and compositional properties of Martian soil and dust: results from Mars Pathfinder. J. Geophys. Res. 105, 1721–1756.

Benkhoff, J., Spohn, T., 1991. Thermal histories of the KOSI samples. Geophys. Res. Lett. 18, 261–264.

Benner, S.A., Devine, K.G., Mateeva, L.N., Powell, D.H., 2000. The missing organic molecues on Mars. Proc. Natl. Acad. Sci. USA 97 (6), 2425–2430.

Biele, J., Ulamec, S., Spohn, T., Mimoun, D., Lognonné, P., Gep Team, 2007. GEP-ExoMars: a geophysics and environment observatory on Mars. In: Lunar and Planetary Institute Conference Abstracts, vol. 38, March, p. 1587–+.

Carter, J.L., McKay, D.S., Taylor, L.A., Carrier, W.D., 2004. Lunar Simulants: JSC-1 is gone; the need for new standardized root simulants. In: Space Resources Roundtable VI, p. 15–+.

Christensen, P.R., Bandfield, J.L., Hamilton, V.E., Ruff, S.W., Kieffer, H.H., Titus, T.N., Malin, M.C., Morris, R.V., Lane, M.D., Clark, R.L., Jakosky, B.M., Mellon, M.T., Pearl, J.C., Conrath, B.J., Smith, M.D., Clancy, R.T., Kuzmin, R.O., Roush, T., Mehall, G.L., Gorelick, N., Bender, K., Murray, K., Dason, S., Greene, E., Silverman, S., Greenfield, M., 2001. Mars global surveyor thermal emission spectrometer experiment: investigation description and surface science results. J. Geophys. Res. 106, 23823–23872.

Christensen, P.R., Bandfield, J.L., Bell, J.F., Gorelick, N., Hamilton, V.E., Ivanov, A., Jakosky, B.M., Kieffer, H.H., Lane, M.D., Malin, M.C., McConnochie, T., McEwen, A.S., McSween, H.Y., Mehall, G.L., Moersch, J.E., Nealson, K.H., Rice, J.W., Richardson, M.I., Ruff, S.W., Smith, M.D., Titus, T.N., Wyatt, M.B., 2003. Morphology and composition of the surface of Mars: Mars Odyssey THEMIS results. Science 300, 2056–2061.

Corbel, C., Hamram, S., Ney, R., Plettemeier, D., Dolon, F., Jeangeot, A., Ciarletti, V., Berthelier, J., 2006. WISDOM: an UHF GPR on the Exomars mission. AGU Fall Meeting Abstracts, December, p. D1218+.

Federico, C., Di Lellis, A.M., Fonte, S., Pauselli, C., Reitz, G., Beaujean, R., 2007. EXOMARS IRAS (DOSE) radiation measurements. Mem. Soc. Astron. Ital. (Suppl. 11), 178–+.

Formisano, V., Angrilli, F., Arnold, G., Atreya, S., Bianchini, G., Biondi, D., Blanco, A., Blecka, M.I., Coradini, A., Colangeli, L., Ekonomov, A., Esposito, F., Fonti, S., Giuranna, M., Grassi, D., Gnedykh, V., Grigoriev, A., Hansen, G., Hirsh, H., Khatuntsev, I., Kiselev, A., Ignatiev, N., Jurewicz, A., Lellouch, E., Lopez Moreno, J., Marten, A., Mattana, A., Maturilli, A., Mencarelli, E., Michalska, M., Moroz, V., Moshkin, B., Nespoli, F., Nikolsky, Y., Orfei, R., Orleanski, P., Orofino, V., Palomba, E., Patsaev, D., Piccioni, G., Rataj, M., Rodrigo, R., Rodriguez, J., Rossi, M., Saggin, B., Titov, D., Zasova, L., 2005. The planetary Fourier spectrometer (PFS) onboard the European Mars Express mission. Planet. Space Sci. 53, 963–974.

Garry, J.R.C., ten Kate, I.L., Martins, Z., Nornberg, P., Ehrenfreund, P., 2006. Analysis and survival of amino acids in martian regolith analogs. Meteorit. Planet. Sci. 41 (3), 391–405.

Greeley, R., 1979. Silt–clay aggregates on Mars. J. Geophys. Res. 84, 6248–6254.

Greeley, R., Iversen, J.D., 1985. Wind as a geological process on Earth, Mars and Venus and Titan. Cambridge Planetary Science Series. Cambridge Univ. Press.

Greeley, R., Wilson, G., Coquilla, R., White, B., Haberle, R., 2000. Windblown dust on Mars: laboratory simulations of flux as a function of surface roughness. Planet. Space Sci. 48, 1349–1355.

Greeley, R., Squyres, S.W., Arvidson, R.E., Bartlett, P., Bell, J.F., Blaney, D., Cabrol, N.A., Farmer, J., Farrand, B., Golombek, M.P., Gorevan, S.P., Grant, J.A., Haldemann, A.F.C., Herkenhoff, K.E., Johnson, J., Landis, G., Madsen, M.B., McLennan, S.M., Moersch, J., Rice, J.W., Richter, L., Ruff, S., Sullivan, R.J., Thompson, S.D., Wang, A., Weitz, C.M., Whelley, P., 2004. Wind-related processes detected by the spirit Rover at Gusev Crater, Mars. Science 305, 810–821.

Griffiths, A.D., Coates, A.J., Jaumann, R., Michaelis, H., Paar, G., Barnes, D., Josset, J.-L., 2006. The Pancam Team, Context for the ESA ExoMars rover: the Panoramic Camera (PanCam) instrument. Int. J. Astrobiol. 5, 269–275.

Gunnlaugsson, H.P., Worm, E.S., Bertelsen P. Goetz W. Kinch, K., Madsen, M.B., Nørnberg P. 2005. Simulations of the magnetic properties experiment on Mars exploration rovers. Hyp. Int. 166, 555–560.

Gunderson, K., Lüthi, B., Russel, P., Thomas, N., 2006. Visible/NIR radiometric signatures of liquid water in martian regolith simulant. Geophys. Res. Abstr. 8, 06578.

Hamelin, M., Szego, K., Godefroy, M., Berthelier, J.-J., Simoes, F., The Ares Team, 2006. ARES: an atmospheric electricity instrument proposed for EXOMARS. Results of balloon tests in the terrestrial atmosphere. In: European Planetary Science Congress, 2006, p. 528+.

Hapke, B., 1993. Theory of Reflectance and Emittance Spectroscopy. Cambridge University Press, Cambridge.

Helbert, J., Jessberger, E., Benkhoff, J., Arnold, G., Banaszkiewicz, M., Bischoff, A., Blecka, M., Calcutt, S., Coangeli, L., Coradini, A., Erard, S., Fonti, S., Killen, R., Knollenberg, J., Kührt, E., Mann, I., Mall, U., Moroz, L., Peter, G., Rataj, M., Robinson M.S. Spohn, T., Sprague, A., Stöffler, D., Taylor, F., Warrell, J., 2005. MERTIS—a thermal infrared imaging spectrometer for the Bepi-Colombo Mission. In: Mackwell, S., Stansbery, E. (Eds.), 36th Annual Lunar and Planetary Science Conference, March, p. 1753–+.

Herkenhoff, K.E., Squyres, S.W., Arvidson, R., Bass, D.S., Bell, J.F., Bertelsen, P., Cabrol, N.A., Gaddis, L., Hayes, A.G., Hviid, S.F., Johnson, J.R., Kinch, K.M., Madsen, M.B., Maki, J.N., McLennan, S.M., McSween, H.Y., Rice, J.W., Sims, M., Smith, P.H., Soderblom, L.A., Spanovich, N., Sullivan, R., Wang, A., 2004. Textures of the soils and rocks at Gusev Crater from Spirit's Microscopic Imager. Science 305, 824–827.

Huguenin, R.L., Miller, K.J., Harwood, W.S., 1979. Frost-weathering on Mars—experimental evidence for peroxide formation. J. Mol. Evol. 14, 103–132.

Johnson, J.R., Grundy, W.M., Shepard, M.K., 2004. Visible/near-infrared spectrogoniometric observations and modeling of dust-coated rocks. Icarus 171, 546–556.

Johnson, J.B., Hopkins, M.A., Kaempfer T. Moore, J.M., Sullivan, R.J., Richter, L., Schmit, N., Athena Science Team, 2007. Progress developing techniques for determining Mars Soil properties from laboratory tests, discrete element modeling, and Mars trenching experiments. In: Lunar and Planetary Institute Conference Abstracts, vol. 38, March, p. 1706–+.

Kinch, K.M., Merrison, J.P., Gunnlaugsson, H.P., Bertelsen, P., Madsen, M.B., Nørnberg, P., 2006. Preliminary analysis of the MER magnetic properties experiment using a computational fluid dynamics model. Planet. Space Sci. 54, 28–44.

Klosky, J.L., Sture, S., Ko, H.-Y., Barnes, F., 1996. Mechanical properties of JSC-1 lunar regolith simulant. In: Engineering, Construction, and Operations in Space V, pp. 680–688.

Marlow, J.J., Martins, Z., Sephton, M.A., 2008. Mars on Earth: soil analogues for future Mars missions. Astron. Geophys. 49, 2.20–2.23.

Marzo, G.A., Bellucci, G., Fonti, S., Saggin, B., Alberti, E., Altieri, F., Politi, R., Zasova, L., The MIMA Team, 2006. MIMA: Mars Infrared MApper—the Fourier spectrometer for the ESA Pasteur/ExoMars rover mission. In: 36th COSPAR Scientific Assembly. COSPAR, Plenary Meeting, vol. 36, p. 1245–+.

Maturilli, A., Helbert, J., Witzke, A., Moroz, L., 2006. Emissivity measurements of analogue materials for the interpretation of data from PFS on Mars Express and MERTIS on Bepi-Colombo. Planet. Space Sci. 54 (11), 1057–1064.

Maturilli, A., Helbert, J., Moroz, L., 2008. The Berlin emissivity database (BED). Planet. Space Sci. 56 (3–4), 420–425.

McKay, D.S., Blacic, J.D. (Eds.), 1991. Workshop on Production and Uses of Simulated Lunar Materials.

McKay, D.S., Carter, J.L., Boles, W.W., Allen, C.C., Allton, J.H., Mar. 1993. JSC-1: a new lunar regolith simulant. In: Lunar and Planetary Institute Conference Abstracts, pp. 963–964.

McKay, D.S., Carter, J.L., Boles, W.W., Allen, C.C., Allton, J.H., 1994. JSC-1: s new lunar regolith simulant. In: Engineering, Construction, and Operations in Space IV, pp. 857–866.

Mendez, C., Garza, E., Gulati, P., Morris, P.A., Allen, C.C., 2005. Isolation and identification of microorganisms in JSC Mars-1 simulant soil. In: lpsc, pp. 2360–+.

Merrison, J., Jensen, J., Kinch, K., Mugford, R., Nørnberg, P., 2004. The electrical properties of Mars analogue dust. Planet. Space Sci. 52, 279–290.

Merrison, J.P., Bertelsen, P., Frandsen, C., Gunnlaugsson, P., Knudsen, J.M., Lunt, S., Madsen, M.B., Mossin, L.A., Nielsen, J., Nørnberg, P., Rasmussen, K.R., Uggerhøj, E., 2002.Simulation of the Martian dust aerosol at low wind speeds. J. Geophys. Res., 107 (E12), 5133, doi:10.1029/2001JE001807.

Möhlmann, D.T.F., 2004. Water in the upper martian surface at mid- and low-latitudes: presence, state, and consequences. Icarus 168, 318–323.

Mustard, J.F., Bell, J.F., 1994. New composite reflectance spectra of Mars from 0.4 to 3.14 micron. Geophys. Res. Lett. 21, 353–356.

Nørnberg, P., Schwertmann, U., Stabjek, H., Andersen, T., Gunnlaugsson, H.P., 2004. Mineralogy of a burned soil compared with four anomalously red quaternary deposits in Denmark. Clay Miner. 39, 85–98.

Oró, J., Holzer, G., 1979. The photolytic degradation and oxidation of organic compounds under simulated Martian conditions. J. Mol. Evol. 14, 153–160.

Parnell, J., Cullen, D., Sims, M.R., Bowden, S., Cockell, C.S., Court, R., Ehrenfreund, P., Gaubert, F., Grant, W., Parro, V., Rohmer, M., Sephton, M., Stan-Lotter, H., Steele, A., Toporski, J., Vago, J., 2007. Searching for life on Mars: selection of molecular targets for ESA's Aurora ExoMars Mission. Astrobiology 7, 578–604.

Patel, M.R., Zarnecki, J.C., Leese, M.R., Towner, M.C., Muller, C., Depiesse C. Moreau D. Gillotay D. Chakrabarti S. 2006. The UV–Vis spectrometer for the ExoMars mission. In: 36th COSPAR Scientific Assembly. COSPAR, Plenary Meeting, vol. 36, p. 2354–+.

Peeters, Z., Quinn, R., Martins, Z., Becker, L., Brucato, J.R., Willis, P., Grunthaner, F., Ehrenfreund, P., 2008. Mars regolith analogues—interactions between mineralogical and organic compounds. In: Lunar and Planetary Institute Conference Abstracts, vol. 39, March, p. 1742–+.

Presley, M.A., Christensen, P.R., 1997a. Thermal conductivity measurements of particulate materials 1. A review. J. Geophys. Res. 102, 6535–6550.

Presley, M.A., Christensen, P.R., 1997b. Thermal conductivity measurements of particulate materials 2. results. J. Geophys. Res. 102, 6551–6566.

Presley, M.A., Christensen, P.R., 2006a. The effect of bulk density on the thermal conductivity of particulate materials under Martian atmospheric pressures. In: Mackwell, S., Stansbery, E. (Eds.), 37th Annual Lunar and Planetary Science Conference, March, p. 2383–+.

Presley, M.A., Craddock, R.A., 2006b. Thermal conductivity measurements of particulate materials: 3. Natural samples and mixtures of particle sizes. J. Geophys. Res. (Planets) 111, 9013.

Quinn, R.C., Zent, A.P., Grunthaner, F.J., Ehrenfreund, P., Taylor, C.L., Garry, J.R.C., 2005. Detection and characterization of oxidizing acids in the Atacama desert using the Mars oxidation instrument. Planet. Space Sci. 53, 1376–1388.

Richter, L., Gromov, V., Josset, J.-L., Möhlmann, D., Nadalini, R., Neuhaus, D., Popp, J., Re, E., Seiferlin, K., Sheridan, S., Sims, M., Spohn, T., Hofer, S., Stuffler, T., Tokano, T., 2003. Development of instrumented moles for in situ subsurface measurements on planetary missions. In: Tools and Technologies for Future Planetary Explorations, 37th ESLAB Symposium.

Richter, L., Schmitz, N., Weiss, S., Mer/Athena Team, 2006. Inferences of strength of soil deposits along MER rover traverses. In: European Planetary Science Congress 2006, p. 523–+.

Seiferlin, K., Spohn, T., Benkhoff, J., 1995. Cometary ice texture and the thermal evolution of comets. Adv. Space Res. 15 (10), 35–38.

Seiferlin, K., Kömle, N.I., Kargl, G., 1996. Line heat-source measurements of the thermal conductivity of porous H_2O ice, CO_2 ice and mineral powders under space conditions. Planet. Space Sci. 44 (7), 691–704.

Seiferlin, K., Chakraborty, S., Gunderson, K., Lüthi, B., Piazza, D., Rieder, M., Sigrist, M., Thomas, N., Weigel, T., 2007. A lightweight reflective baffle for the Bepi-Colombo laser altimeter: manufacture. Opt. Eng. (SPIE) 46 (4), 043003-1–043003-11.

Soderblom, L.A., Anderson, R.C., Arvidson, R.E., Bell, J.F., Cabrol, N.A., Calvin, W., Christensen, P.R., Clark, B.C., Economou, T., Ehlmann, B.L., Farrand, W.H., Fike, D., Gellert, R., Glotch, T.D., Golombek, M.P., Greeley, R., Grotzinger, J.P., Herkenhoff, K.E., Jerolmack, D.J., Johnson, J.R., Jolliff, B., Klingelhöfer, G., Knoll, A.H., Learner, Z.A., Li, R., Malin, M.C., McLennan, S.M., McSween, H.Y., Ming, D.W., Morris, R.V., Rice, J.W., Richter, L., Rieder, R., Rodionov, D., Schröder, C., Seelos, F.P., Soderblom, J.M., Squyres, S.W., Sullivan, R., Watters, W.A., Weitz, C.M., Wyatt, M.B., Yen, A.,

Zipfel, J., 2004. Soils of Eagle Crater and Meridiani Planum at the opportunity rover landing site. Science 306, 1723–1726.
Southworth, B.A., Voelker, B.M., 2003. Hydroxyl radical production via the photo-fenton reaction in the presence of fluvic acid. Environ. Sci. Technol. 37, 1130–1136.
Spohn, T., Ball, A.J., Seiferlin, K., 2001a. HP3: a heat flow and physical properties package for the surface of mercury. In: The Royal Astronomical Society Meeting Mercury: What We Know and What We Don't.
Spohn, T., Seiferlin, K., Kömle, N.I., Kargl, G., Hagermann, A., 2001b. The HP3 package for the Bepi-Colombo lander. Geophys. Res. Abstr. 3, 7369.
Spohn, T., Lognonne, P., Dehant, V., Giardini, D., Friis-Christensen, E., Calcutt, S., The Gep Team, A., 2006. GEP, A Geophysical and Environmental integrated payload for ExoMars. In: European Planetary Science Congress, 2006, p. 592–+.
Steiner, G., Kömle, N.I., 1991. A model of the thermal conductivity of porous water ice at low gas pressures. Planet. Space Sci. 39, 507–513.
Stoker, C.R., Bullock, M.A., 1997. Organic degradation under simulated Martian conditions. J. Geophys. Res. 102, 10881–10888.
Taylor, L.A., McKay, D.S., Carrier, W.D., Carter, J.L., Weiblen, P., 2004. The nature of lunar soil: considerations for simulants. In: Space Resources Roundtable VI, p. 46–+.
Ten Kate, I.L., Garry, J.R.C., Peeters, Z., Quinn, R., Foing, B., Ehrenfreund, P., 2005. Amino acid photostability on the Martian surface. Meteorit. Planet. Sci. 40, 1185–1194.
Barnes, D., Battistelli, E., Bertrand, R., Butera, F., Chatila, R., Biancio, A., Draper, C., Ellery, A., Gelmi, R., Ingrand, F., Koeck, C., Lacroix, S., Lamon, P., Lee, C., Magnani, P., Patel, N., Pompei, C., Re, E., Richter, L., Rowe, M., Siegwart, R., Slade, R., Smith, M.F., Terrien, G., Wall, R., Ward, R., Waugh, L., Woods, M., The Rover Team, 2006. The ExoMars rover and Pasteur payload phase A study: an approach to experimental astrobiology. Int. J. Astrobiol. 5, 221–241.
Ulamec, S., Biele, J., Lognonne, P., Mimoun, D., Spohn, T., 2006. A geophysics environmental package for Mars: proposed design for the Exomars Mission. In: 36th COSPAR Scientific Assembly. COSPAR, Plenary Meeting, vol. 36, p. 946–+.
Vago, J., Gardini, B., Kminek, G., Baglioni, P., Gianfiglio, G., Santovincenzo, A., Bayón, S., van Winnendael, M., 2006. Exo-Mars—searching for life on the Red Planet. ESA Bull. 126, 16–23.
Vago, J.L., Kminek, G., Baglioni, P., Gardini, B., McCoy, D., Gianfiglio, G., Exomars Project Team, 2007. Upcoming science activities in support of ESA's ExoMars Mission. In: Lunar and Planetary Institute Conference Abstracts, March, vol. 38, p. 1001–+.
Walling, C., 1975. Fenton's reagent revisited. Acc. Chem. Res. 8, 125–131.
Weiblen, P.W., Gordon, K., 1988. Characteristics of a simulant for lunar surface materials. LPI Contrib. 652, 254.
Weiblen, P.W., Murawa, M.J., Reid, K.J., 1990. Preparation of simulants for lunar surface materials. In: Engineering, Construction, and Operations in Space II, pp. 98–106.
Wieczorek, M.A., Spohn, T., The HP3 Instrument Team, 2007. The heat flow of the Moon: what do we know, and how do we measure it? In: AGU Fall Meeting Abstracts, December, C2+.
Yen, A.S., Kim, S.S., Hecht, M.H., Frant, M.S., Murray, B., 2000. Evidence that the reactivity of the Martian soil is due to superoxide ions. Science 289, 1909–1912.
Zent, A.P., McKay, C.P., 1994. The chemical reactivity of the martian soil and implications for future missions. Icarus 108, 146–157.
Zöhrer, A., Kargl, G., 2006. Finite element modelling of penetration tests into martian analogue materials. In: ESA SP-607, p. P5.6.